Heuristic Approach for Arrival Management of eVTOLs in On-Demand Urban Air Mobility

Priyank Pradeep * and Peng Wei †

Iowa State University, Ames, IA, 50011

The arrival sequencing and scheduling problem have been formulated in the urban air mobility (UAM) context for homogeneous and mixed fleets of eVTOLs (winged/wingless) expected to land on a vertiport. In this paper, a novel UAM airspace design concept has been proposed to separate arrival air traffic of wingless eVTOLs from winged eVTOLs until merging at the metering fix. Two separate vertiport arrival procedures have also been proposed for the problem based on anticipated UAM traffic density in emergent (low) and early expanded (moderate/high) operations, as proposed by NASA. The objective of the problem is to minimize the makespan (landing completion time) of a given set of eVTOLs. A heuristic approach called insertion, and local search (ILS) combined with two different scheduling methods: i) mixed-integer linear programming (MILP) and ii) time-advance (TA) are proposed to minimize the makespan of the mixed fleet of eVTOLs. Next, the impact of the number of landing pads (N) on the makespan is studied to aid in early expanded UAM operations. Finally, sensitivity analysis is performed to see the impact of the following on the sequencing and scheduling algorithms: i) the number of eVTOLs expected to land (n) and ii) the number of eVTOLs used in the local neighborhood search (k). Through numerical simulations and sensitivity analysis, our algorithms demonstrated real-time scheduling capabilities; therefore, it can be potentially used for on-demand UAM arrival operations. *

Nomenclature

E(i)	Earliest time of arrival of the i^{th} eVTOL aircraft
ETA(i)	Estimated time of arrival of the i^{th} eVTOL aircraft
ILS	Insertion and local search heuristic method
k	Number of free (moving window) eVTOL aircraft involved in each local neighborhood search
L(i)	Latest time of arrival of the i^{th} eVTOL aircraft
MF	Metering fix

*Ph.D. Candidate, Aerospace Engineering Department, Howe Hall, 537 Bissell Rd and AIAA Student Member.

†Assistant Professor, Aerospace Engineering Department, Howe Hall, 537 Bissell Rd and AIAA Senior Member.

*Presented as Paper in 2018 IEEE/AIAA 37th Digital Avionics Systems Conference (DASC), London, 2018, pp. 1-7, doi: 10.1109/DASC.2018.8569225.

MG Metering gate

MILP Mixed-integer linear programming

n Number of eVTOLs expected to land on a vertiport

N Number of landing pads on a vertiport

RTA(i) Required time of arrival of the i^{th} eVTOL aircraft

TA Time-advance strategy

$t_v(i)$ Time of vertical descent of the i^{th} eVTOL aircraft

Δt_{ij} Minimum time separation between the trailing eVTOL aircraft (j) and the leading eVTOL aircraft (i) at the metering fix

TOD Top of descent

I. INTRODUCTION

Commuting time has an adverse impact on physical activity and cardio-respiratory fitness (CRF) of human beings [1]. In 2014, road-traffic congestion resulted in wastage of 6.9 billion person-hours and 3.1 billion gallons of excess fuel consumed in the USA alone [2]. On-demand passenger electric vertical takeoff and landing (eVTOL) aircraft are perceived as the key enabler for urban air mobility (UAM) to cut down on daily commute time for people and reduce carbon footprint by utilizing three-dimensional airspace efficiently with zero operational emission [3–8].

Recently, technological advances have made it possible to build and flight test eVTOL aircraft [3, 7, 9]. Over a dozen companies, for example, Airbus A^3, Aurora Flight Sciences, EHang, Joby Aviation, Kitty Hawk, Leonardo, Lilium, Terrafugia, Volocopter, etc., with many different design approaches, are passionately working to make eVTOLs a reality. Despite various designs, they all have distributed electric propulsion (DEP) system in common. Considerable power-to-weight, efficiency, reliability and operational flexibility improvements are possible utilizing DEP technology in eVTOLs compared to the rotor system of conventional helicopters [3, 7, 9–11]. The conventional helicopters are capable of VTOL, but the noise generated by them has been significant enough to compel communities to take legal action on their usage in UAM [7]. DEP powered eVTOLs have a higher downwash velocity compared to conventional helicopters that permits a more rapid vertical descent without entering a vortex ring state [3]. Engine failure accounts for 18 % of general aviation accidents when combined with fuel management errors. The use of DEP, controllers, and a redundant battery bus architecture avoids the problems of catastrophic engine failure by having full propulsion system redundancy [3, 9, 10]. The eVTOLs also have an advantage of zero operational emissions as they use electric propulsion [3, 9, 15].

To realize the UAM dream, orders of magnitude more aircraft than that operate today in the current airspace would be required to serve the urban public in the metropolitan areas [8]. Significant resources have been invested toward builders of takeoff and landing areas (TOLA), and researchers of the airspace integration concepts, technologies, and procedures needed to conduct UAM operations safely and efficiently alongside other airspace users [7]. In this paper, we focus on eVTOL aircraft arrival sequencing and scheduling for the following UAM traffic: i) emergent operations (low traffic density) and ii) early expanded operations (moderate/high traffic density) [7, 14] to aid in UAM airspace design.

II. BACKGROUND AND MOTIVATION

A. Background

The envisioned concept of UAM involves a network of eVTOL aircraft that will enable rapid and reliable transportation between suburbs and downtowns of cities, and within cities (intra-city) [3, 8]. Similar to Unmanned Aircraft System Traffic Management (UTM), the air traffic services for UAM need to safely and efficiently manage eVTOL aircraft without burdening Air Traffic Control (ATC) or impacting traditional aviation operations [8, 15]. However, unlike the small UAV that can take off and land almost anywhere in the UTM framework, eVTOL aircraft of UAM operation need to take off from and land at vertiports.

From our previous research on trajectory optimization of eVTOLs, we learned that arrival air traffic flow needs to be separated for wingless (multirotor) eVTOL aircraft from winged (tilt-rotor/tandem tilt-wing) eVTOL aircraft because of difference in cruise speeds [4–6]. For example, the cruise speed of multirotor eVTOL aircraft EHang 184 is 27.78 m/s, whereas the minimum maneuver speed of Airbus Vahana (tandem tilt-wing eVTOL) is 50 m/s [9, 12, 13]. Hence, it would be a big challenge for eVTOL arrival sequencing and scheduling service provider to safely and efficiently maintain minimum time separation between the wingless and winged eVTOLs, especially when winged eVTOL is trailing the wingless on the same airway in UAM. Therefore, we propose an airspace design concept to separate wingless eVTOL arrival air traffic from winged until merging at the metering fix because of the reason mentioned above.

B. Motivation

Before the large-scale fully autonomous UAM operations become true, the first bottleneck of UAM traffic throughput is expected to appear at the vertiport (or skyport) terminal airspace. In UAM operations, we anticipate that the arrival phase (compared with departure) will be one of the most safety-critical phases of flight. This is because of the following reasons: i) arrival traffic will be restricted by the capacity of vertiports, and air traffic is, in general, dynamic and complex in terminal airspace; ii) flight endurance of eVTOL aircraft will be limited by the specific energy (the amount of energy per unit weight provided by the battery) and state-of-charge (SOC) of lithium-ion polymer (Li-Po) batteries [3, 4]. Therefore, UAM operations will require safe and efficient services similar to ATC services in National Airspace System (NAS) for commercial aircraft [3, 8]. However, matured UAM operations will require introducing orders of magnitude more aircraft (mainly air taxis) in the National Airspace System (NAS) then that is accommodated by the current air traffic control (ATC) system in the US [7, 8].

Our research on solving the arrival sequencing and scheduling for eVTOL aircraft in UAM is inspired by deterministic modeling of arrival sequencing and scheduling problem in the terminal area for commercial air traffic [16–18, 21–25]. First-come-first-served (FCFS), is the most straightforward arrival sequencing and scheduling method as it schedules the aircraft in the order of their estimated time of arrival (ETA) to the metering points (gates and runway threshold) [18]. The FCFS sequencing order provides a sense of fairness and is easy to implement for the ATC. However, it can not achieve optimal/near-optimal runway throughput in UAM because of very different nominal cruise speeds of different eVTOL aircraft types. Therefore, mixed fleet of eVTOLs (winged/wingless) and the low specific energy of Li-Po batteries provides an incentive to deviate from the FCFS order and find the most efficient sequence (landing order) with optimal spacing between the eVTOL aircraft to maximize vertiport throughput for UAM arrival operations.

Finding an optimal arrival sequencing order is a non-deterministic polynomial-time (NP) hard problem [22–25, 28–30]. Hence, instead of finding an exact solution for sequencing order, many researchers have investigated heuristic and metaheuristic optimization algorithms for commercial air traffic [22–25, 28–30]. Furthermore, due to the anticipated dynamic environment of on-demand UAM operations, it might not be possible to compute the optimal arrival sequence of eVTOLs that deviates significantly from the FCFS order in real-time. However, we anticipate that arrival sequencing and scheduling service provider for UAM will have the computing capability to explore other sequences by shifting eVTOL landing slots by a small number from its FCFS order like the commercial aircraft in the terminal area [22–25, 29, 31]. This paper aims to solve eVTOL arrival sequencing and scheduling problem in UAM using insertion and local search (ILS) heuristic approach [22].

In the commercial air traffic world, one possible approach to decrease the average delay incurred by aircraft and maximize the runway throughput is to accelerate from their ideal speeds. This strategy is known as time advance (TA) [18, 23–25]. Similarly, to maximize the throughput at a vertiport, given the anticipated randomness in on-demand traffic in UAM and different cruise speeds of various eVTOLs, time-advance (TA) strategy [18, 23–25] has been combined with the ILS in this paper.

III. PROBLEM STATEMENTS FOR EMERGENT AND EARLY EXPANDED UAM OPERATIONS

In this research, the ground infrastructure of the vertiport is assumed to be as follows: i) takeoff pads are separated from landing pads [20]; ii) departure operations are independent of arrival operations [20]; iii) the ratio of the number of gates and staging stands to the number of landing pads is optimal to support immediate taxi-in of an eVTOL aircraft to a gate or staging stand after the touchdown on the landing pad [20] and iv) UAM arrival routes (lateral and vertical paths) are fixed.

DEP powered eVTOLs have a higher downwash velocity than conventional helicopters that permit a more rapid

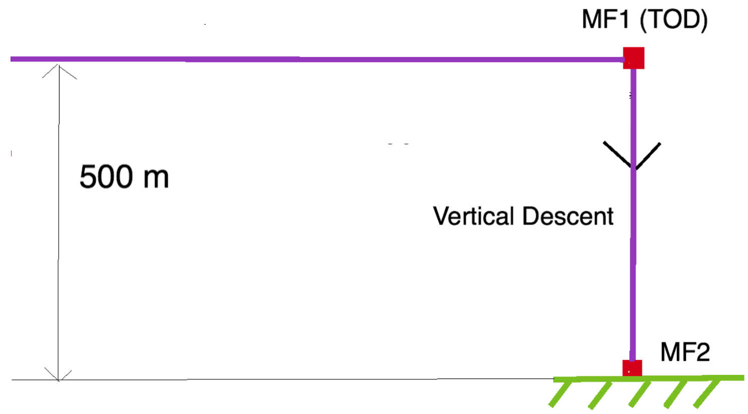

Fig. 1 Vertical view of eVTOL aircraft arrival on a vertiport with single landing pad

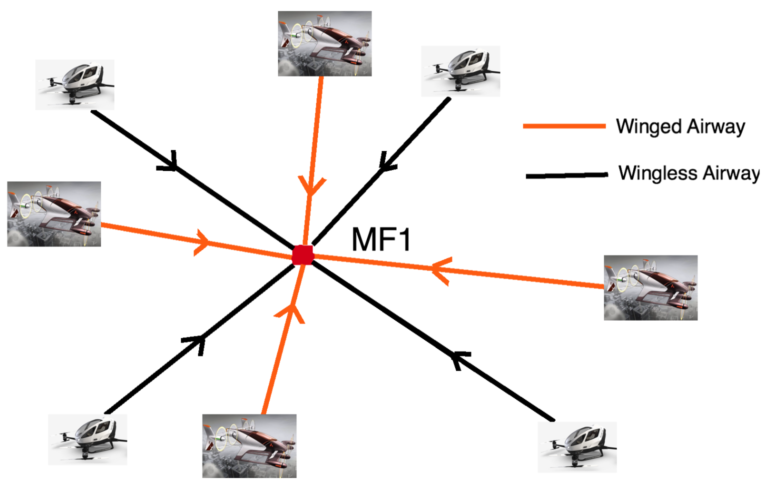

Fig. 2 Lateral view of UAM arrival airspace in low traffic density flow

vertical descent without entering a vortex ring state [2]. Therefore, eVTOLs are better suited for vertical descent than conventional helicopters. Moreover, the vertical descent would be exceptionally safe when skyscrapers surround the vertiport. Hence, the descent is assumed to be vertical descent for both emergent (low traffic density) and early expanded (moderate/high traffic density) UAM operations, as shown in Fig. 1.

A. CONOPs for eVTOL aircraft arrival in emergent UAM operations

For emergent UAM operations (low traffic density) [7], the arrival concept of operations (CONOPs) for the mixed fleet of eVTOL aircraft (wingless/winged) is assumed to be cruising at a constant altitude followed by the vertical descent to land on the vertiport with a single landing pad. For low traffic density CONOPs, we assumed the first metering fix (MF1) for arrival at cruise altitude directly above the vertiport and the second metering fix (MF2) at the vertiport itself.

In this paper, we propose a novel UAM airspace design concept to separate wingless eVTOL arrival air traffic from winged until merging at the metering fix. This is because of the considerable difference in cruise speeds of winged and wingless eVTOLs [9, 12, 13]. Therefore, the arrival routes (airways) for winged eVTOL aircraft are separated from the arrival routes (airways) of wingless eVTOL aircraft, as shown in Fig. 2.

The ETA for each eVTOL aircraft to the MF1 is assumed to be based on the following: i) nominal cruise speed of the eVTOL aircraft, ii) negligible time to decelerate to hover, and iii) no miles-in-trail enroute restrictions on the airways. The ETA for the i^{th} eVTOL aircraft to the MF2 is given by:

$$ETA(i)_{\text{MF2}} = ETA(i)_{\text{MF1}} + t_v(i) \quad \forall\, i \tag{1}$$

where $t_v(i)$ is the time taken by the i^{th} eVTOL aircraft to descent vertically from the cruise altitude to the landing pad. Since the MF1 is also a merging point for eVTOL air traffic in UAM, therefore, the (ETA)s of eVTOL aircraft to the MF1 is used to define the FCFS order.

B. CONOPs for eVTOL aircraft arrival in early expanded UAM operations

For early expanded UAM operations (moderate/high traffic density) [7], the arrival concept of operations (CONOPs) for the mixed fleet of eVTOL aircraft (wingless/winged) is assumed to be cruising at a constant altitude followed by the descent (from fixed TOD) to land on the vertiport with single or multiple landing pads [20]. Similar to the low traffic density UAM operations, the arrival routes (airways) for winged eVTOL are separated from the arrival routes (airways) of wingless eVTOLs because of difference in cruise speeds of winged and wingless eVTOLs [9, 12, 13]. However, we propose an airspace design concept to merge wingless and winged eVTOL aircraft arrival traffic at a metering gate (MG), as shown in Fig. 3 and Fig. 4. The waypoints located at the boundary of the terminal area of radius 400 m surrounding the vertiport, as shown in Fig. 3 and Fig. 4 are referred to as (MG)s [19]. The (MG)s are used as a means of controlling the UAM traffic flow rate into the vertiport during moderate and high traffic conditions [19]. We assumed 400 m radius for the terminal region because it is sufficient to allow both winged and wingless to slow down from nominal cruise speed to hover with deceleration less than g/3.

In this research, for early expanded UAM operations, we assumed the first metering fix (MF1) for arrival at cruise altitude directly above the centroid of the topology of landing pads and the second metering fix (MF2) at the centroid itself. Given the safety requirement of minimum horizontal spacing of 200 ft between the centerline of landing pads (even for simultaneous descent operations of helicopters) [20], the descent from the MF1 (TOD) to any of the landing pads is approximated by a vertical descent.

As stated, the location of MF1 (TOD) is assumed to be as defined in Table 1 and shown in Fig. 3 and Fig. 4 for a vertiport with different number of landing pads. The ETA for each eVTOL aircraft to the MF1 is assumed to be based on the following: i) nominal cruise speed of the eVTOL aircraft until sequencing a MG, ii) lateral paths from

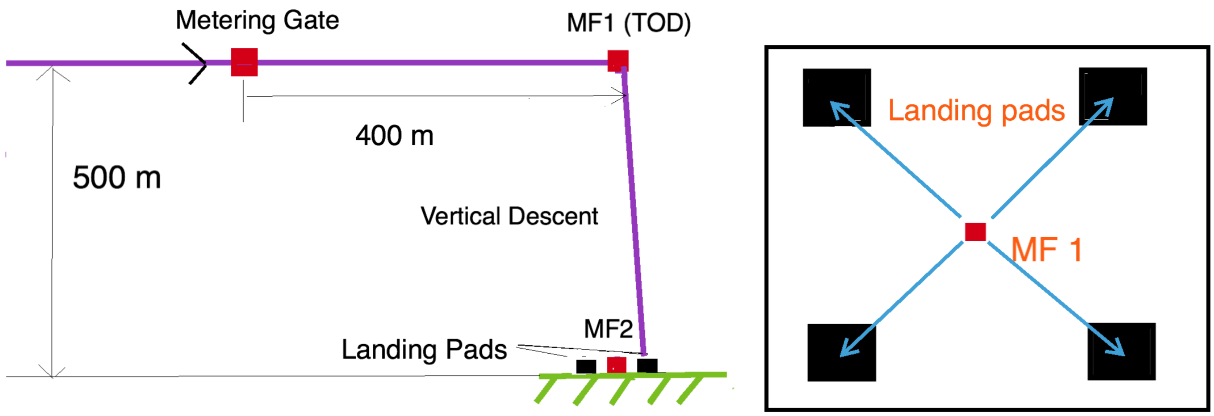

Fig. 3 Vertical view of eVTOL aircraft arrival and top view of vertiport with four landing pads

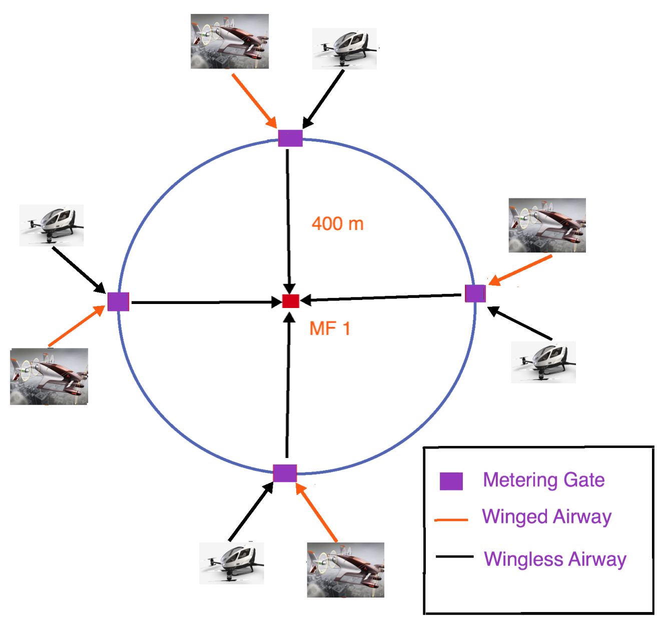

Fig. 4 Lateral view of UAM arrival airspace in high traffic density flow

Table 1 Topology of landing pad(s) on a vertiport

Number of Landing Pad(s)	Topology
1	Point (center of the landing pad)
2	Line (center of each landing pad is placed at the end point)
3	Equilateral triangle (center of each landing pad is placed at the vertex)
4	Square (center of each landing pad is placed at the vertex)
5	Regular pentagon (center of each landing pad is placed at the vertex)
6	Regular hexagon (center of each landing pad is placed at the vertex)

(MG)s to the MF1 are considered geodesic path, iii) same transition time to travel from a MG to the MF1 for both types of eVTOLs even though winged eVTOLs travel faster than wingless eVTOLs, but winged eVTOLs have to undergo configuration change whereas wingless eVTOLs maintains the same configuration for vertical descent [3–7, 9], and iv) no miles-in-trail enroute restrictions on the airways. The ETA for the i^{th} eVTOL aircraft to the MF1 is given by:

$$ETA(i)_{\text{MF1}} = ETA(i)_{\text{MG}} + t(i)_{\text{transition}} \quad \forall\, i \tag{2}$$

$$ETA(i)_{\text{MF2}} = ETA(i)_{\text{MF1}} + t_v(i) \quad \forall\, i \tag{3}$$

where $t(i)_{\text{transition}}$ is the transition time for the i^{th} eVTOL to travel from a MG to the MF1 while decelerating to hover at the MF1 and $t_v(i)$ is the time taken by the i^{th} eVTOL aircraft to descent vertically from the cruise altitude to the landing pad. Since the boundary of the terminal area is also a merging point for early expanded UAM air traffic, therefore, the (ETA)s of eVTOL aircraft to an MG is used to define the FCFS order.

C. Objective of the problem

The goal of a scheduler is to assign each aircraft in the arrival traffic a required time of arrival (RTA) to the metering fix. However, for safety the RTA(i) for the i^{th} eVTOL aircraft should lie between it's earliest time of arrival (E(i)) and latest time of arrival (L(i)) to the metering fix. In general, the earliest time of arrival of an eVTOL aircraft is calculated based on the maximum operating speed (VMO) of the aircraft. In contrast, the latest time of arrival is calculated based on the state-of-charge (SOC) of the on-board Li-Po battery pack of the eVTOL aircraft.

We anticipate that the arrival sequencing and scheduling service providers for eVTOL aircraft would like to land the sequence of eVTOLs as soon as possible, given the limitations with Li-Po batteries and safety concerns associated with air traffic congestion in the terminal area. The optimization problem of minimizing the makespan i.e. the RTA of the last eVTOL (in the mixed fleet) to the MF1 is equivalent to maximizing vertiport throughput [22–25]. Hence, the objective of this research is to find the eVTOL aircraft landing order heuristically for a given set of mixed fleet of eVTOLs such that the makespan of the eVTOLs (n) expected to land is minimized. Therefore, the decision variables are the set of (RTA)s to the MF1 and the objective of the problem is to minimize the RTA of the last eVTOL aircraft to the MF1.

In order to minimize the RTA of the last eVTOL aircraft to the MF1 (makespan) the following two objective functions are used separately in the proposed algorithm:

$$min. RTA(n)_{\text{MF1}} \tag{4a}$$

$$min. \sum_{i=1}^{n} RTA(i)_{\text{MF1}} \tag{4b}$$

where i denotes the i^{th} aircraft in the arrival traffic sequence and n is the total number of eVTOLs in the fleet. Therefore, the makespan of the fleet of eVTOLs is numerically minimized using either of the following two objective functions in the proposed algorithm: i) the RTA of the last eVTOL aircraft in the arrival sequence (equation 4a) and ii) the summation of RTAs of all eVTOLs (equation 4b).

D. Window constraints on arrival scheduling

For both operations (emergent and early expanded), the following window constraints are imposed on the $RTA(i)_{\mathrm{MF1}}$ of each eVTOL aircraft, where i denotes the i^{th} aircraft in the arrival traffic sequence:

$$E(i)_{\mathrm{MF1}} \leq RTA(i)_{\mathrm{MF1}} \leq L(i)_{\mathrm{MF1}} \quad \forall\, i \tag{5}$$

E. Minimum time separation in emergent operations

As emergent UAM operations are anticipated to involve low altitude operations [2, 7, 9, 12] with low air-traffic density, therefore, we assumed vertiport with a single landing pad. Therefore, we imposed a safety requirement that the trailing eVTOL aircraft shall not descend unless the leading has landed on the vertiport. Hence, the minimum time separation (Δt_{ij}) between the trailing eVTOL aircraft j and the leading eVTOL aircraft i is dependent on the time ($t_v(i)$) taken by the leading eVTOL aircraft (i) to descent vertically from the cruise altitude to the landing pad and is independent of the trailing eVTOL aircraft (j).

$$\Delta t_{ij} = t_v(i) \quad \forall\, i < j \tag{6}$$

Therefore, the following constraints have been imposed on the eVTOL sequencing and scheduling problem:

$$t_v(i) \leq RTA(j)_{\mathrm{MF1}} - RTA(i)_{\mathrm{MF1}} \quad \forall\, i < j \tag{7}$$

In this paper, the vertical descent is assumed to be from the cruise altitude of 500 m above sea-level to the vertiport at sea-level. The time of vertical descent ($t_v(i)$) for winged and wingless eVTOLs is computed using the multiphase optimal control framework (minimum energy path) from our previous research on trajectory optimization of Airbus Vahana and EHang 184 respectively [4–6]. The multiphase optimal control problem is transcribed using GPOPS-II, and then IPOPT has been used as the solver to solve the problem transcribed to nonlinear programming by GPOPS-II [32, 33].

Table 2 Minimum time separations (sec) at the MF1

Leading eVTOL \ Trailing eVTOL	Winged	Wingless
Winged	151	151
Wingless	173	173

F. Minimum time separation in early expanded operations

The maximum capacity of a conventional airport is proportional to the following: i) the number of runways, ii) airport runway design efficiency factor, iii) the number of gates and their utilization factor, and iv) aircraft separation factor (a function of aircraft type) [34].

In this research, as shown in Fig. 3, the vertiports are assumed to have multiple landing pads to support early expanded operations (moderate/high traffic density). As stated earlier, the vertiport capacity is assumed to be not limited by parking and staging gates. This is based on the assumption that the ratio of the number of gates and staging stands to the number of landing pads is optimal to support immediate taxi-in of an eVTOL aircraft after the touchdown on the landing pad [20]. Therefore, in analogy to the conventional airport, the arrival capacity of a vertiport is proportional to the number of landing pads (N) at the vertiport [20, 35]. Hence, we imposed the minimum time separation (Δt_{ij}) between the trailing eVTOL aircraft j and the leading eVTOL aircraft i at the MF1 (as shown in equation 8) based on the following: i) time of vertical descent ($t_v(i)$) of the leading eVTOL aircraft (i); ii) inversely proportional to the number of landing pads (N) on the vertiport which implies benefits of using multiple landing pads at a vertiport; and iii) lower bound of 45 seconds on the minimum time of separation at the MF1 is per the maximum arrival flow rate at the vertiport (1 flight in every 45 seconds) [14]:

$$\Delta t_{ij} = max(45, \frac{t_v(i)}{\mathrm{N}}) \quad \forall\ i < j \tag{8}$$

where $t_v(i)$ is as defined in Table 2.

Therefore, the following constraints have been imposed on the eVTOL sequencing and scheduling problem:

$$\Delta t_{ij} \leq RTA(j)_{\mathrm{MF1}} - RTA(i)_{\mathrm{MF1}} \quad \forall\ i < j \tag{9}$$

IV. PROPOSED ALGORITHM

A. Insertion and local search heuristics

The insertion and local search (ILS) heuristic algorithm developed in this paper for arrival sequencing and scheduling of eVTOL aircraft expected to land on a vertiport with single and multiple landing pads, is based on the ILS algorithm described for single runway scheduling of commercial air traffic by Malik and Jung [22].

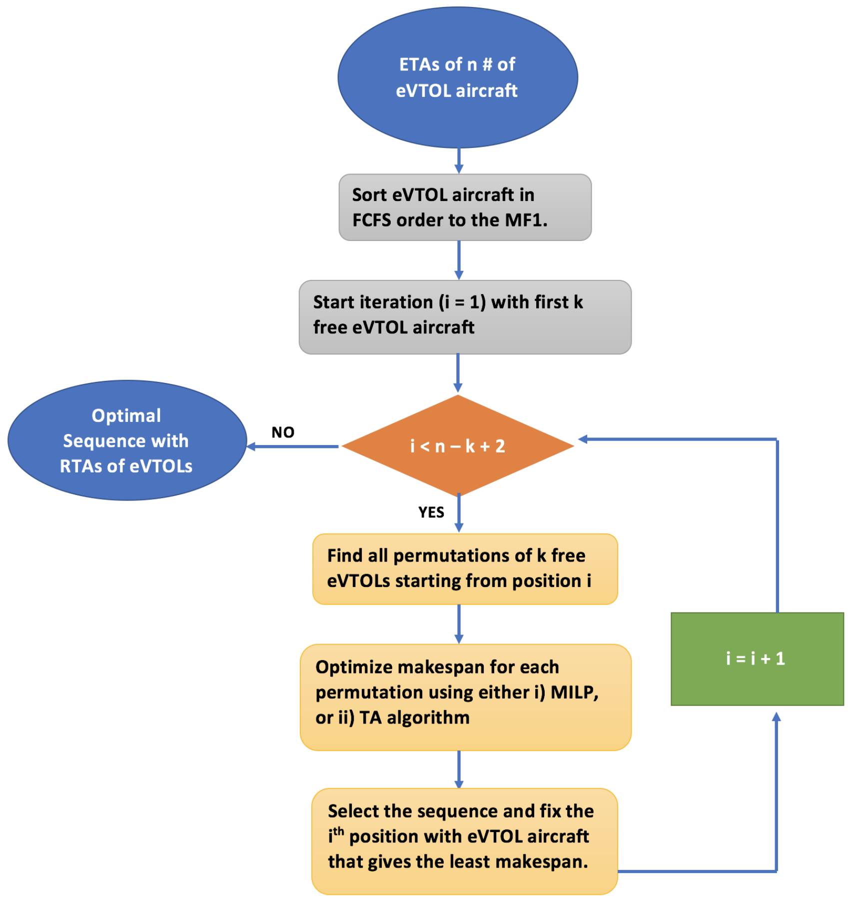

Fig. 5 Block diagram of arrival sequencing and scheduling

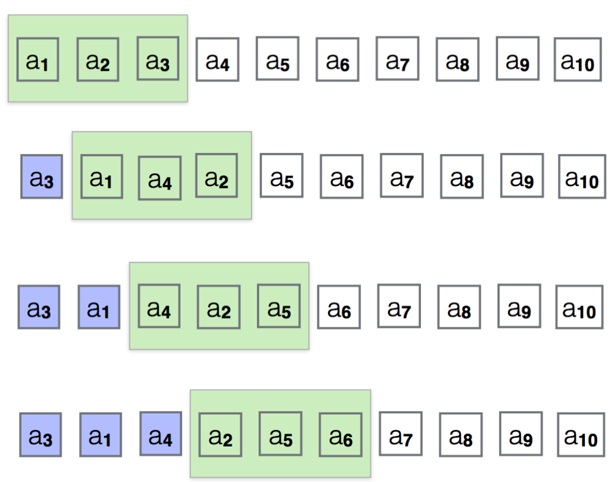

Fig. 6 Example of ILS (k=3) algorithm for eVTOL arrival sequencing and scheduling [22]

The heuristic starts with the initial guess for eVTOL aircraft arrival sequence as the FCFS to the MF1. In this paper, the term position implies landing position of an eVTOL aircraft in the arrival sequence. The iteration begins for fixing the 1^{st} position in the arrival sequence and then it continues until fixing the $(n - k + 1)^{th}$ position, where n is the total number of eVTOL aircraft expected to land on the vertiport and k is the number of free (moving window of free) eVTOL aircraft involved in each iteration for local neighborhood search (local optimization). For example, the i^{th} iteration for fixing the i^{th} position in the arrival sequence involves local neighborhood search starting from the i^{th} position in the sequence till the $(i + k - 1)^{th}$ position. Hence, at each iteration $k!$ sequences (permutations) of eVTOL aircraft are possible. Therefore, local optimization is carried out $k!$ times to pick the preferred local sequence and fix the i^{th} position with the best eVTOL aircraft. During the local neighborhood search, the preferred sequence is the one with the least objective value among all the objective values in the $k!$ sequences. Hence, after the i^{th} iteration, the eVTOL aircraft positions from 1^{st} till i^{th} are considered fixed whereas the positions from $(i + 1)^{th}$ till n^{th} are considered free. However, at the end of fixing the $(n - k + 1)^{th}$ position, the eVTOL aircraft positions at $n + 2 - k, ..., n$ are fixed based on the preferred sequence for $(n - k + 1)^{th}$ position in the arrival sequence, as shown in Fig. 5.

Consider a feasible sequence (H) consisting of n eVTOL aircraft $(a_1, a_2, a_3, ...a_n)$. For example, when $k = 3$, six different sequences $(H_i^1, H_i^2, H_i^3, H_i^4, H_i^5, H_i^6)$ are possible during the i^{th} iteration by juggling eVTOL aircraft located at free neighborhood positions: $i, i + 1$ and $i + 2$ [22]. Fig. 6, shows a few iteration steps of the ILS algorithm for $k = 3$ and fleet of 10 eVTOL aircraft expected to land, starting with the FCFS order. The green highlight indicates the preferred sequence of k free eVTOL aircraft during the i^{th} iteration that fixes the eVTOL aircraft for the i^{th} position in the sequence. The preferred sequence is the one with the least objective value among all the six possibilities during the local neighborhood search. Finally, the i^{th} position (blue box in Fig. 6) in the arrival sequence is fixed using the eVTOL aircraft at the i^{th} position in the preferred sequence during the iteration.

As stated in the previous section, the eVTOL aircraft arrival sequencing and scheduling problem's objective function is to minimize the RTA to the MF1 of the last eVTOL aircraft in the arrival sequence. The optimal objective value for each sequence in a given iteration is computed using either the MILP solver Gurobi Optimizer [36] or in-house developed time advance (TA) algorithm [18, 19, 23–25]. In the current research, ILS-TA and ILS-MILP methods are used mainly for performing speed change maneuvers. Therefore, other air traffic management strategies like altitude change maneuvers, path stretch, or holding patterns are not considered for the minimization of the makespan of the mixed fleet of eVTOLs.

B. TA algorithm

Time-advance (TA) is an effective method of reducing the average delay time without changing the order of the aircraft. In this method, the benefits of speeding up an aircraft during periods of heavy traffic in order to reduce gaps that naturally occur in the FCFS schedules is recognized [18, 19, 23–25]. Therefore, the main idea behind the TA algorithm in the UAM context is to speed-up an eVTOL whenever the separation from the leading eVTOL is larger than the minimum time separation (Δt_{ij}). However, in this research TA algorithm is used only for local neighborhood search/optimization as part of ILS algorithm (shown in Fig. 5 and Fig. 6).

The $RTA(j)_{MF1}$ for the j^{th} eVTOL aircraft trailing behind the i^{th} eVTOL aircraft is given by:

$$RTA(j)_{\mathrm{MF1}} = max\{E(j)_{\mathrm{MF1}}, RTA(i)_{\mathrm{MF1}} + \Delta t_{ij}\} \ \forall \ i < j \tag{10}$$

Also, for the feasibility of the solution, the (RTA)s of all eVTOL aircraft to the MF1 should be less than their corresponding latest times of arrival to the MF1.

V. NUMERICAL SIMULATIONS

We anticipate arrival air traffic to a vertiport at random time distribution because of the on-demand nature of UAM but at an average rate when viewed as a group for a set of eVTOLs expected to land on a vertiport. Therefore, we simulated the estimated times of arrival (ETA)s of eVTOL aircraft using the Poisson arrival process [37] using Python 3.6 (high-level programming language) [38] on MacBook Pro with 2.8 GHz Intel Core i7 processor. In this research, irrespective of air traffic density (emergent or early expanded), we simulated two types of eVTOL air traffic, i.e., winged and wingless, arriving via different airways and merging at the MF1 or MG depending upon arrival procedure (traffic density), as shown in Fig. 2 and Fig. 4.

In this research, the winged eVTOL aircraft are simulated per the performance characteristics of Airbus Vahana

Table 3 Performance data of eVTOL aircraft

eVTOL Type	Nominal Cruise Speed (m/s)	VMO (m/s)
Winged	50	80
Wingless	27.77	33.33

[5, 9]. In contrast, wingless eVTOL aircraft are simulated per the performance characteristics of EHang 184 [4, 12], as shown in Table 3.

A. Numerical simulations for emergent operations

For emergent operations (low traffic density), the earliest time of arrival of each eVTOL to the MF1 is calculated by ignoring transition and hover time. Therefore, the earliest time of arrival ($E(i)$) of the i^{th} eVTOL aircraft to the MF1 is calculated based on the maximum speed of the eVTOL aircraft as follows:

$$E(i)_{\mathrm{MF1}} = \frac{V_{\mathrm{cruise}}}{VMO} * ETA(i)_{\mathrm{MF1}} \quad \forall \ i \tag{11}$$

where V_{cruise} is the nominal cruise speed and VMO is the maximum operating speed of the eVTOL aircraft.

The latest time of arrival ($L(i)$) of the i^{th} eVTOL aircraft to the MF1 should be ideally calculated based on the CONOPs and state-of-charge (SOC) of the Li-Po battery pack of the eVTOL aircraft [26, 27]. However, because of the unavailability of Li-Po battery model, in this paper, we used the random function to simulate the effect of CONOPs and SOC of the Li-Po battery pack on the ETA of an eVTOL:

$$L(i)_{\text{MF1}} = ETA(i)_{\text{MF1}} + U(t) \quad \forall\, i \tag{12}$$

where $U(t)$ is a random function that uniformly samples a value between 900 and 1200 seconds. In this research, we assumed values (between 900 to 1200 seconds) so that the eVTOL has enough state-of-charge (SOC) to reach an alternate vertiport (if required) in the Dallas Fort Worth Metropolitan area [39] in case of the destination vertiport closure.

B. Numerical simulations for early expanded operations

For early expanded operations (moderate/high traffic density), the earliest time of arrival of each eVTOL to the boundary of terminal area (a MG) of the vertiport is calculated by assuming maximum cruise speed of the eVTOL. Therefore, the earliest time of arrival ($E(i)$) of the i^{th} eVTOL aircraft to a MG is as follows:

$$E(i)_{\text{MG}} = \frac{V_{\text{cruise}}}{VMO} * ETA(i)_{\text{MG}} \quad \forall\, i \tag{13}$$

where V_{cruise} is the nominal cruise speed and VMO is the maximum operating speed of the eVTOL aircraft.

The earliest time of arrival ($E(i)$) of the i^{th} eVTOL aircraft to the MF1 is as follows:

$$E(i)_{\text{MF1}} = E(i)_{\text{MG}} + t_{\text{transition}} \tag{14}$$

In this paper, the transition time ($t_{\text{transition}}$) is assumed to be 30 seconds for both eVTOL types. The assumption is based on passenger comfort, therefore, limiting the absolute value of deceleration in the terminal area to less than g/3 (where g is the acceleration due to gravity).

The latest time of arrival ($L(i)$) of the i^{th} eVTOL aircraft to the boundary of terminal area (a MG) should be ideally calculated based on the CONOPs and state-of-charge (SOC) of the Li-Po battery pack of the eVTOL aircraft [26, 27]. However, because of the unavailability of Li-Po battery model, in this paper, we used the random function to simulate the effect of CONOPs and SOC of the Li-Po battery pack on the ETA of an eVTOL:

$$L(i)_{\text{MG}} = ETA(i)_{\text{MG}} + U(t) \quad \forall\, i \tag{15}$$

where $U(t)$ is a random function which uniformly samples a value between 900 and 1200 seconds. We assumed values (between 900 to 1200 seconds) so that the eVTOL has enough SOC to reach the destination vertiport and then alternate vertiport (if required) in the Dallas Fort Worth Metropolitan area [39] in case of the destination vertiport closure.

The latest time of arrival ($L(i)$) of the i^{th} eVTOL aircraft to the MF1 is assumed as follows:

$$L(i)_{\text{MF1}} = L(i)_{\text{MG}} + t_{\text{transition}} \tag{16}$$

VI. CASE STUDIES AND RESULTS

A. Case studies and results of emergent operations

The proposed heuristic methods (ILS-MILP and ILS-TA) to minimize the makespan (RTA of the last eVTOL to the MF1) of a given set of eVTOLs are written in Python 3.6 and run on MacBook Pro with 2.8 GHz Intel Core i7 processor. In this research, we assumed the Poisson arrival process for emergent operations (low traffic density) with an arrival rate of 10 eVTOL aircraft expected to land in 1800 seconds on a vertiport with a single landing pad. Our assumption of approximately 3 minutes interval between landing is based on the minimum time separation enforced at the MF1 for safe emergent operations (equations 6 and 7), which in turn is based on the time of vertical descent (Table 2).

We considered the following case studies to understand the impact of (i) minimum time separation, (ii) resequencing and (iii) time-advance strategy on the makespan of homogeneous and mixed fleets of eVTOLs under non-emergency flight conditions:

- Homogeneous fleet:
  - For each eVTOL in the homogeneous fleet, ETA is simulated using the Poisson arrival process.
  - Initially, eVTOLs are assumed to be flying at nominal cruise speed without minimum time separation enforced between them (at the MF1) following the FCFS landing order (sequence) based on (ETA)s.
  - Next, the makespan of the fleet is computed by enforcing minimum time separation (Table 2) between eVTOLs at the MF1. The makespan is computed using the FCFS landing order but without applying heuristic algorithms (ILS-MILP and ILS-TA).
  - Finally, the makespan of the fleet is minimized heuristically using ILS-MILP and ILS-TA algorithms under a constrained environment (Equation 5 and Table 2) using objective function 1 (equation 4a).
- Mixed fleet:
  - For each eVTOL in the mixed fleet, ETA is simulated using the Poisson arrival process.
  - Initially, eVTOLs are assumed to be flying at nominal cruise speed without minimum time separation enforced between them (at the MF1) following the FCFS landing order (sequence) based on (ETA)s.
  - Next, the makespan of the fleet is computed by enforcing minimum time separation (Table 2) between

eVTOLs at the MF1. The makespan is computed using the FCFS landing order but without applying heuristic algorithms (ILS-MILP and ILS-TA).

- Next, the makespan of the fleet is minimized using TA algorithm under a constrained environment (Equation 5 and Table 2). However, the FCFS landing order is still maintained.
- Finally, the makespan of the fleet is minimized heuristically using ILS-MILP and ILS-TA algorithms under a constrained environment (Equation 5 and Table 2) using both objective functions (equations 4a and 4b) separately. Therefore, the makespan and landing order are computed by heuristic algorithms.

1. Homogeneous fleet - (a) fleet mix ratio (10/0) and (b) fleet mix ratio (0/10)

In this case study, the same set of (ETA)s to the MF1 are simulated for both fleets (winged and wingless). The (ETA)s are generated using the Poisson arrival process, assuming a total time interval of 1800 seconds for the following: (a) 10 winged and 0 wingless, and (b) 0 winged and 10 wingless.

From Table 4 and Table 5, we can observe that the makespan computed for both fleets by enforcing only minimum

Table 4 Homogeneous fleet of winged eVTOLs (a): simulation and results of ILS-MILP and ILS-TA methods

Simulation	Minimum Time Separation Enforced	Heuristic Results using Objective Function 1			
ETA (Sec)	RTA (Sec)	Sequence (ILS-MILP)	RTA (Sec)	Sequence (ILS-TA)	RTA (Sec)
270	270	1	169	1	169
356	421	2	320	2	320
386	572	3	471	3	471
823	823	4	622	4	622
1110	1110	5	773	5	773
1247	1261	6	924	6	924
1406	1412	7	1075	7	1075
1584	1584	8	1226	8	1226
1689	1735	9	1377	9	1377
1694	1886	10	1528	10	1528

Table 5 Homogeneous fleet of wingless eVTOLs (b): simulation and results of ILS-MILP and ILS-TA methods

Simulation	Minimum Time Separation Enforced	Heuristic Results using Objective Function 1			
ETA (Sec)	RTA (Sec)	Sequence (ILS-MILP)	RTA (Sec)	Sequence (ILS-TA)	RTA (Sec)
270	270	1	225	1	225
356	443	2	398	2	398
386	616	3	571	3	571
823	823	4	744	4	744
1110	1110	5	925	5	925
1247	1283	6	1098	6	1098
1406	1456	7	1271	7	1271
1584	1629	8	1444	8	1444
1689	1802	9	1617	9	1617
1694	1975	10	1790	10	1790

time constraints between eVTOLs at the MF1 and without applying time advance strategy is a safe but inefficient method because of large temporal spacing between some of the eVTOLs.

Using both methods (ILS-MILP and ILS-TA), the makespan computed is the same for a given homogeneous fleet, i.e., 1528 seconds for winged eVTOLs and 1790 seconds for wingless eVTOLs respectively. However, the heuristic results show that instead of minimization of the makespan from the initial value of 1694 seconds for a homogeneous fleet of wingless eVTOLs, it increased to 1790 seconds to maintain the minimum time separation between eVTOLs at the MF1. The higher value of the makespan of the wingless fleet compared to the winged fleet is because of the larger minimum time separation constraint at the MF1 and lower cruise speeds i.e., nominal and VMO (Table 2).

From Table 4 and Table 5, we can also observe that resequencing is not beneficial for a homogeneous fleet of eVTOLs under non-emergency flight conditions.

2. Mixed fleet - ratio (5/5)

In this case study, the (ETA)s of 5 winged and 5 wingless eVTOL aircraft are generated separately using the Poisson arrival process, assuming a total time interval of 1800 seconds, as shown in Table 6.

From Table 6 and Table 7, we can observe that for the simulated mixed fleet of eVTOLs, both methods (ILS-MILP

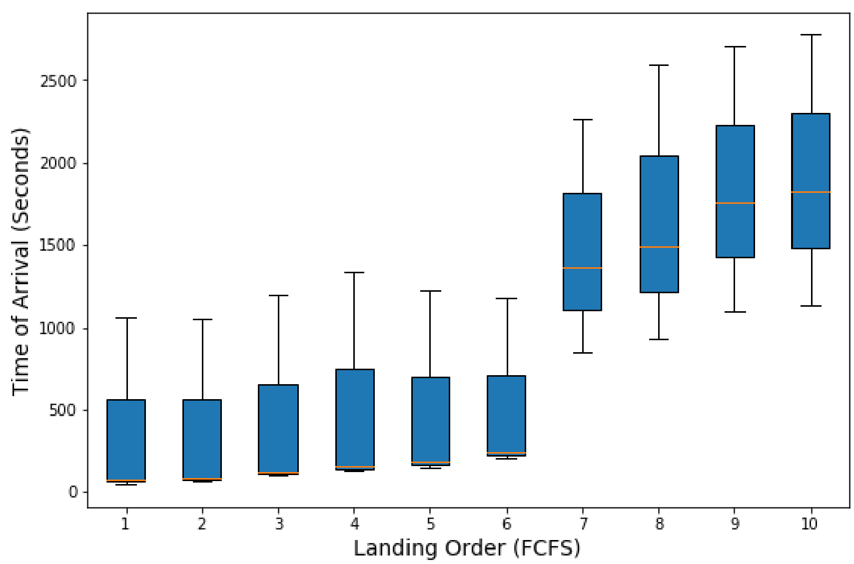

Fig. 7 Mixed fleet - ratio (5/5): box plots using earliest, estimated and latest times of arrival of each eVTOL

and ILS-TA) using two different objective functions (equation 4a and equation 4b), minimized the makespan (RTA of the last eVTOL to the MF1) to the same value (1517.68 seconds). The minimization of the makespan is achieved by speeding-up eVTOLs whenever possible without violating any constraints. Also, it can be seen that for this simulation, the preferred landing order (sequence) remained FCFS. The box plots in Fig. 8 are plotted using the earliest time of arrival, estimated time of arrival, and latest time of arrival of each eVTOL in the mixed fleet. The FCFS landing order of the mixed fleet can be justified by: i) the minimum values (earliest times of arrival of eVTOLs to the MF1) of box plots in ascending order, and ii) temporal separation between estimated times of arrival of eVTOLs at position 6 and position 7 much higher than minimum time separation constraint at the MF1.

We observed the computational time of ILS-MILP method is higher than ILS-TA method, as shown in Table 8. For example, using objective function 1 (equation 4a), ILS-MILP computed the heuristic results (landing order and (RTA)s) in 0.729 seconds, whereas ILS-TA method computed the heuristic results in 0.012 seconds and 0.013 seconds using objective function 1 (equation 4a) and objective function 2 (equation 4b) respectively.

Table 6 Mixed fleet - ratio (5/5): simulation of eVTOLs and results upon time constraint enforcement

Simulation		Minimum Time Separation Enforced
eVTOL Type	ETA (Sec)	FCFS Order RTA (Sec)
Winged	77.88	77.88
Wingless	82.82	228.88
Wingless	119.38	401.88
Wingless	157.40	574.88
Wingless	183.93	747.88
Wingless	245.64	920.88
Winged	1361.62	1361.62
Winged	1493.70	1512.62
Winged	1759.36	1759.36
Winged	1820.91	1910.36

Table 7 Mixed fleet - ratio (5/5): results of ILS-MILP and ILS-TA methods using two different objective functions

TA Algorithm	Heuristic Results using Objective Function 1		Heuristic Results using Objective Function 2	
FCFS Order RTA (Sec)	ILS-MILP/ILS-TA Sequence	ILS-MILP/ILS-TA RTA (Sec)	ILS-MILP/ILS-TA Sequence	ILS-MILP/ILS-TA RTA (Sec)
48.68	1	48.68	1	48.68
199.68	2	199.68	2	199.68
372.68	3	372.68	3	372.68
545.68	4	545.68	4	545.68
718.68	5	718.68	5	718.68
891.68	6	891.68	6	891.68
1064.68	7	1064.68	7	1064.68
1215.68	8	1215.68	8	1215.68
1366.68	9	1366.68	9	1366.68
1517.68	10	1517.68	10	1517.68

Table 8 Mixed fleet - ratio (5/5): comparison of computational time (seconds)

ILS-TA (Objective Function 1)	ILS-TA (Objective Function 2)	ILS-MILP (Objective Function 1)
0.012	0.013	0.729

3. Mixed fleet - ratio (7/3)

In this case study, the (ETA)s of 7 winged and 3 wingless eVTOL aircraft are generated separately using the Poisson arrival process, assuming a total time interval of 1800 seconds, as shown in Table 9.

From Table 9 and Table 10, we can observe that for the simulated mixed fleet of eVTOLs, both methods (ILS-MILP and ILS-TA) minimized the makespan (RTA of the last eVTOL to the MF1) to the same value (1604.48 seconds) irrespective of the objective function (equation 4a or equation 4b). The minimization of the makespan can be attributed to the change in the landing order (resequencing) and speeding-up eVTOLs whenever possible without violating any constraints. Also, the makespan (1786.18 seconds) of the mixed fleet after applying TA strategy and enforcing constraints but maintaining the FCFS landing order (i.e., without resequencing) is higher than the makespan (1604.48 seconds) after applying TA strategy with the change in landing order (resequencing).

The multiple shuffles in landing order (resequencing) shows priority given to winged eVTOLs compared to wingless eVTOLs for minimization of the makespan because of the faster cruise speed of the former. For example, with both objective functions, the initial landing order (6) of the wingless eVTOL is changed to the landing order (9) after applying heuristic algorithms. However, objective function 2 (equation 4b) i.e., the summation of all (RTA)s, did additional shuffle (i.e., between position 2 and position 3) in the initial landing order. Therefore, objective function 2 seems to be more efficient than objective function 1. This can also be visualized from the minimum values (earliest times of arrival to the MF1) of box plots in Fig. 8.

Additionally, we can observe from Table 10 and Fig. 8 that irrespective of the objective function, the heuristic landing order is not the same as landing order based on the earliest times of arrival. For example, the earliest time of arrival of the eVTOL initially at position 6 (heuristic position 9) is higher than that of the eVTOL initially at position 10 (heuristic position 10), as shown in Fig. 8.

Again, we observed the computational time of ILS-MILP method is higher than ILS-TA method, as shown in Table 14. For example, using objective function 1, ILS-MILP method computed the heuristic results (landing order and (RTA)s) in more time (0.702 seconds) compared to ILS-TA method (0.013 seconds). It can also be seen that for ILS-TA method, computational time using objective function 2 (0.016 seconds) is comparable to the computational time using objective function 1 (0.013 seconds).

4. Mixed fleet - ratio (3/7)

In this case study, the (ETA)s of 3 winged and 7 wingless eVTOL aircraft are generated separately using the Poisson arrival process, assuming a total time interval of 1800 seconds, as shown in Table 12.

From Table 12 and Table 13, we can observe that for the simulated mixed fleet of eVTOLs, both methods (ILS-MILP and ILS-TA) minimized the makespan (RTA of the last eVTOL to the MF1) to the same value for a given objective function i.e. 1735.43 seconds for objective function 1 (equation 4a) and 1713.43 seconds for objective function 2 (equation

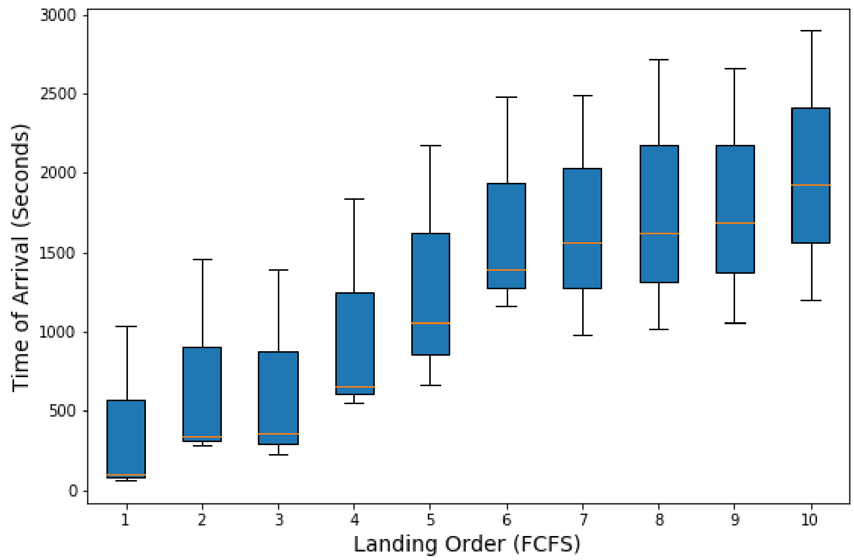

Fig. 8 Mixed fleet - ratio (7/3): box plots using earliest, estimated and latest times of arrival of each eVTOL

Table 9 Mixed fleet - ratio (7/3): simulation of eVTOLs and results upon time constraint enforcement

Simulation		Minimum Time Separation Enforced
eVTOL Type	**ETA (Sec)**	**FCFS Order RTA (Sec)**
Winged	100.31	100.31
Wingless	339.28	339.28
Winged	358.97	512.28
Wingless	657.59	663.28
Winged	1056.93	1056.93
Wingless	1392.26	1392.26
Winged	1565.58	1565.58
Winged	1622.93	1716.58
Winged	1685.24	1867.58
Winged	1921.41	2018.58

Table 10 Mixed fleet - ratio (7/3): results of ILS-MILP and ILS-TA methods using two different objective functions

TA Algorithm	Heuristic Results using Objective Function 1		Heuristic Results using Objective Function 2	
FCFS Order RTA (Sec)	**ILS-MILP/ILS-TA Sequence**	**ILS-MILP/ILS-TA RTA (Sec)**	**ILS-MILP/ILS-TA Sequence**	**ILS-MILP/ILS-TA RTA (Sec)**
62.69	1	62.69	1	62.69
282.72	2	282.72	3	224.36
455.72	3	455.72	2	375.36
606.72	4	606.72	4	548.36
779.72	5	779.72	5	721.36
1160.18	7	978.48	7	978.48
1333.18	8	1129.48	8	1129.48
1484.18	9	1280.48	9	1280.48
1635.18	6	1431.48	6	1431.48
1786.18	10	1604.48	10	1604.48

Table 11 Mixed fleet - ratio (7/3): comparison of computational time (seconds)

ILS-TA (Objective Function 1)	ILS-TA (Objective Function 2)	ILS-MILP (Objective Function 1)
0.013	0.016	0.702

4b). Also, the makespan (1735.43 seconds) of the mixed fleet after applying TA strategy and enforcing constraints but maintaining the FCFS landing order (i.e., without resequencing) is same as the makespan (1735.43) computed using objective function 1 (equation 4a) and applying TA strategy with the change in landing order (resequencing). Therefore, a single shuffle in landing order, i.e., positions 8 and 9 in this case study using objective function 1 (equation 4a), did not yield the benefit over the FCFS landing order in minimizing the makespan. Also, from the box plots in Fig. 9, it can be observed that though the earliest time of arrival of winged eVTOL initially positioned at landing order 5 (initially) is lower than the earliest times of arrival of eVTOLs in initial positions 2, 3 and 4. Still, the two methods (ILS-MILP and ILS-TA) using objective function 1 (equation 4a), did not reshuffle their positions. This result can be attributed to the fact that objective function 1 (equation 4a) is inefficient in reshuffling positions of eVTOLs early in the landing order to minimize the makespan.

Clearly, from Table 12 and Table 13, we can also observe that the makespan (1713.43 seconds) computed using objective function 2 (equation 4b) is lower than the makespan (1735.43 seconds) using objective function 1 (equation 4a). This result can be attributed to the fact that objective function 2 (equation 4b) is more effective in resequencing eVTOLs early in the landing order efficiently based on the earliest times of arrival i.e. allowing winged eVTOLs to speed-up and land earlier whenever possible.

Again, we observed that the computational time of ILS-MILP method is higher than ILS-TA method. For example, using objective function 1, the computational time of ILS-MILP method is 0.743 seconds, whereas the computational time of ILS-TA method is 0.014 seconds. It can also be seen that for ILS-TA method, computational time using objective function 2 (0.017 seconds) is comparable to the computational time using objective function 1 (0.014 seconds).

Table 12 Mixed fleet - ratio (3/7): simulation of eVTOLs and results upon time constraint enforcement

Simulation		Minimum Time Separation Enforced
eVTOL Type	**ETA (Sec)**	**FCFS Order RTA (Sec)**
Wingless	148.90	148.90
Wingless	474.53	474.53
Wingless	539.73	647.53
Wingless	560.09	820.53
Winged	602.34	993.53
Wingless	767.72	1144.53
Wingless	830.62	1317.53
Wingless	960.75	1490.53
Winged	1096.67	1663.53
Winged	1674.03	1814.53

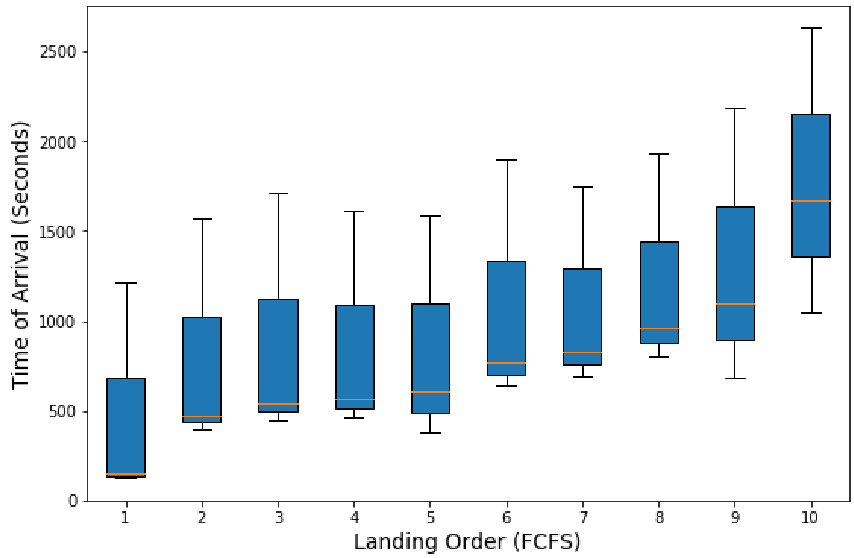

Fig. 9 Mixed fleet - ratio (3/7): box plots using earliest, estimated and latest times of arrival of each eVTOL

Table 13 Mixed fleet - ratio (3/7): results of ILS-MILP and ILS-TA methods using two different objective functions

TA Algorithm	Heuristic Results using Objective Function 1		Heuristic Results using Objective Function 2	
FCFS Order RTA (Sec)	ILS-MILP/ILS-TA Sequence	ILS-MILP/ILS-TA RTA (Sec)	ILS-MILP/ILS-TA Sequence	ILS-MILP/ILS-TA RTA (Sec)
124.08	1	124.08	1	124.08
395.43	2	395.43	2	395.43
568.43	3	568.43	5	568.43
741.43	4	741.43	3	719.43
914.43	5	914.43	4	892.43
1065.43	6	1065.43	6	1065.43
1238.43	7	1238.43	9	1238.43
1411.43	9	1411.43	10	1389.43
1584.43	8	1562.43	7	1540.43
1735.43	10	1735.43	8	1713.43

Table 14 Mixed fleet - ratio (3/7): comparison of computational time (seconds)

ILS-TA (Objective Function 1)	ILS-TA (Objective Function 2)	ILS-MILP (Objective Function 1)
0.014	0.017	0.743

B. Results of early expanded operations

1. Case study IV - impact of number of landing pads (N) on makespan

In this research, for early expanded operations (moderate/high traffic density), we assumed a mixed fleet of 80 eVTOLs expected to land in 3600 seconds on a vertiport with single or multiple landing pads. In this case study, the impact of the number of landing pads (as defined in Table 1) on makespan (arrival throughput) is studied using the proposed ILS-TA heuristic algorithm with k=5 and objective function 1 (equation 4a). The original makespan of the simulated eVTOLs is 3383.21 seconds without imposing the minimum time separation constraint between the eVTOLs at the MF1. The minimum time separation enforced between the eVTOLs using ILS-TA algorithm is per Table 2 and equation 8. Table 15 shows the impact of the number of landing pads (N) on makespan (arrival throughput). From Table 15, it can be seen that with a lower bound on minimum time separation of 45 seconds, the near-optimal result is achieved by using a vertiport with 4 landing pads per MF1 (TOD) for the proposed arrival procedure.

Table 15 Case study IV: impact of number of landing pads (N) on makespan

Number of Landing Pads	Makespan (ILS-TA) (Sec)	Computational Time (Sec)
1	12836.15	28.70
2	6442.65	30.31
3	4311.48	27.37
4	3604.15	25.43
5	3604.15	24.62
6	3604.15	24.11

C. Sensitivity analysis

1. Case study V - impact of number of eVTOLs (n) on computational time

The computational time is calculated for both algorithms, i.e., ILS-MILP and ILS-TA, with k=3 for sequencing and scheduling a different number of eVTOLs (n: 10, 50, 90, 130, 170, 210, 250) arriving at the Poisson arrival rate of 1 eVTOL per 60 seconds to the MF1 (assuming emergent arrival CONOP). In this case study, both the algorithms use objective function 1 (equation 4a) for makespan minimization. As stated earlier, ILS-MILP and ILS-TA are run on MacBook Pro with a 2.8 GHz Intel Core i7 processor. Also, to check the performance of both the algorithms, a lower minimum time separation requirement has been imposed on the arrival air-traffic, i.e., 60 seconds for both types of eVTOLs, and the mixed fleet is assumed to contain an equal mix of winged and wingless eVTOLs. From Fig. 10, it can be seen that ILS-TA algorithm is computationally faster than ILS-MILP. Also, it can be seen that ILS-TA with k=3 algorithm can schedule 250 eVTOLs in less than 10 seconds.

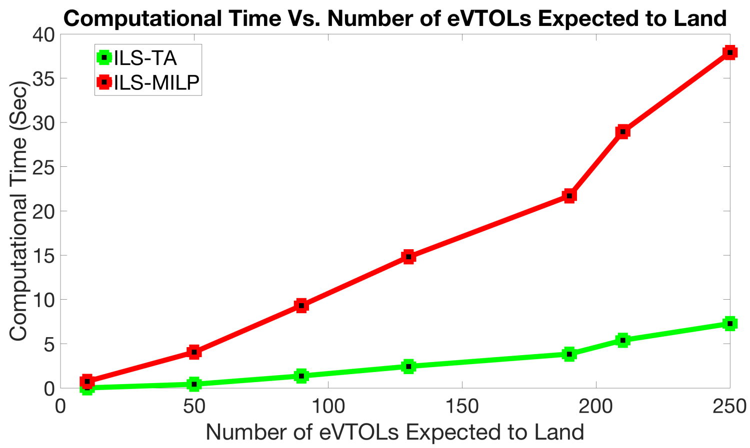

Fig. 10 Case study V: computational time of two algorithms for different number of eVTOLs

2. Case study VI - impact of moving window of free eVTOLs (k) on computational time and makespan

In this case study, the impact of the moving window of free eVTOLs (k) on the computational time and results (makespan of the set of eVTOLs) of ILS-TA algorithm (using objective function 1) is studied. The following UAM air-traffic is simulated for the case study: i) emergent operations: 8 eVTOLs (n) at the Poisson arrival rate of 1 eVTOL per 180 seconds consisting of 4 winged and 4 wingless eVTOLs; ii) early expanded operations: 100 eVTOLs (n) at the Poisson arrival rate of 100 per hour (3600 seconds) consisting of 50 winged and 50 wingless eVTOLs.

The computational time of the algorithm with a different number of moving window of free eVTOLs (k: 3, 4, 5, 6, 7, 8) involved in each local optimization (local neighborhood search) is calculated and compared for emergent operations, as shown in Table 16. Similarly, the results (makespan of the emergent UAM air-traffic) computed using ILS-TA algorithm with different k values are compared, as shown in Table 16. The original makespan of the simulated eVTOLs is 908.92 seconds without imposing the minimum time separation constraint between the eVTOLs. The minimum time separation imposed between the eVTOLs using ILS-TA algorithm is per Table 2. Therefore, from Table 16, the impact of k on the following can be observed: i) the number of local searches per iteration, ii) makespan, and iii) overall computational time of the algorithm.

Table 16 Case study VI a: sensitivity analysis of moving window of free eVTOLs (k) for emergent operations

k	Number of Local Searches	Makespan (ILS-TA) (Sec)	Computational Time (ILS-TA) (ms)
3	6	1170.44	8.93
4	24	1170.44	49.95
5	120	1170.44	212.94
6	720	1170.44	960.66
7	5040	1170.44	6202.86
8	40320	1170.44	47020.0

The computational time of the algorithm with a different number of moving window of free eVTOLs (k: 3, 4, 5, 6,

Table 17 Case study VI b: sensitivity analysis of moving window of free eVTOLs (k) for early expanded operations

k	Number of Local Searches	Makespan (ILS-TA) (Sec)	Computational Time (ILS-TA) (Sec)
2	2	3203.18	0.71
3	6	3174.48	1.37
4	24	3168.59	7.98
5	120	3163.34	39.68
6	720	3162.34	211.24
7	5040	3162.34	1479.08

7) involved in each local optimization (neighborhood search) is calculated and compared for early expanded operations, as shown in Table 17. Similarly, the results (makespan of the early expanded UAM air-traffic) computed using ILS-TA algorithm with different k values are compared, as shown in Table 17. The original makespan of the simulated eVTOLs is 3604.31 seconds without imposing the minimum time separation constraint between the eVTOLs. The minimum time separation imposed between the eVTOLs using ILS-TA algorithm is 30 seconds. Therefore, from Table 17, the impact of k on the following can be observed: i) the number of local searches per iteration, ii) makespan, and iii) overall computational time of the algorithm.

From Table 16 and Table 17, the following can be observed: i) For low density (emergent) operations with approximately 10 or fewer eVTOLs scheduled to land in half an hour, the heuristic algorithm (ILS-TA with k=3) produces the near-optimal results with computational time in milliseconds (8.93 ms); ii) For early expanded operations (moderate/high traffic density) with approximately 100 eVTOLs scheduled to land in an hour, the heuristic algorithm (ILS-TA with K=5) produces the near-optimal results for arrival sequencing and scheduling problem. The results are computed with considerably lower computational time (less than 40 seconds) compared to computational times at higher values of k, i.e., 6, 7, or higher. On the other hand, the heuristic algorithm (ILS-TA with K=3) computes the results (landing order and makespan), though not near-optimal but better than FCFS in less than 2 seconds.

VII. CONCLUSIONS

In this paper, we formulated arrival sequencing and scheduling problem in urban air mobility (UAM) context for homogeneous and mixed fleets of eVTOLs (winged/wingless) expected to land on a vertiport. We proposed a novel UAM airspace design concept to separate wingless eVTOL arrival air traffic from winged until merging at the metering fix because of considerable difference in cruise speeds of winged and wingless eVTOLs. Two separate vertiport arrival procedures have also been proposed for the problem based on anticipated UAM traffic density in emergent (low) and early expanded (moderate/high) operations, as proposed by NASA. The arrival procedure for early expanded operations is proposed based on arrival procedure of emergent operations as a baseline with the addition of metering gates (MG)s on the boundary of the terminal area (a circular area of radius 400 m around a vertiport) and multiple landing pads on the vertiport.

The objective of the problem is to minimize the makespan of a given set of eVTOLs, which is equivalent to maximizing the arrival throughput. The landing order (sequence) and makespan of the mixed fleet are determined using a heuristic approach called insertion and local search (ILS) combined with two different scheduling methods i) mixed-integer linear programming (MILP) or ii) time-advance (TA) algorithm. The heuristic results show that for minimization of the makespan it is essential to: i) speed-up a trailing eVTOL whenever separation from the leading is more than minimum time separation, and ii) winged eVTOLs should have designated airways separate from wingless eVTOLs so that they can overtake earlier landing slot(s) of wingless eVTOLs whenever possible. The makespan results of heuristic algorithms (ILS-TA and ILS-MILP) with k=3, show that objective function 2 (the summation of RTAs of all eVTOLs) produces better or equivalent results when compared with that of objective function 1 (RTA of the last eVTOL).

Upon applying ILS-TA algorithm on simulation of early expanded UAM operations, the results showed the need for multiple landing pads to enable safe and efficient arrival. For a lower bound of 45 seconds on a minimum time of separation at the TOD (MF1) and proposed CONOPs, a vertiport with 4 landing pads is the optimal configuration.

The sensitivity analysis using MacBook Pro with 2.8 GHz Intel Core i7 indicates the following: i) ILS-TA is computationally faster than ILS-MILP and produces the same heuristic results. Also, it can be seen that ILS-TA algorithm with k=3 can schedule 250 eVTOLs in less than 10 seconds; ii) For low density (emergent) operations with approximately 10 or fewer eVTOLs scheduled to land in half an hour, the heuristic algorithm (ILS-TA with k=3) produces the near-optimal results with computational time in milliseconds (8.93 ms); and iii) For early expanded operations (moderate/high traffic density) with approximately 100 eVTOLs scheduled to land in an hour, the heuristic algorithm (ILS-TA with K=5) produces the near-optimal results for arrival sequencing and scheduling problem. The results are computed with considerably lower computational time (less than 40 seconds) compared to computational times at higher values of k, i.e., 6, 7, or higher. On the other hand, the heuristic algorithm (ILS-TA with K=3) computes the results (landing order and makespan), though not near-optimal but better than FCFS in less than 2 seconds.

VIII. Acknowledgments

This research has been partially funded by the National Science Foundation (NSF) Award - 1565979.

References

[1] Hoehner, C. M., Barlow, C. E., Allen, P., and Schootman, M., "Commuting distance, cardiorespiratory fitness, and metabolic risk," American journal of preventive medicine, Vol. 42, No. 6, 2012, pp. 571-578. doi:10.1016/j.amepre.2012.02.020.

[2] Schrank, D., Eisele, B., Lomax, T., and Bak, J., "2015 urban mobility scorecard," `https://static.tti.tamu.edu/tti.tamu.edu/documents/mobility-scorecard-2015.pdf`, 2015. [Online; accessed 18-January-2019].

[3] Uber-Elevate, "Fast-forwarding to a future of on-demand urban air transportation," https://www.uber.com/elevate.pdf/, 2016. [Online; accessed 18-January-2019].

[4] Pradeep, P. and Wei, P., "Energy-Efficient Arrival with RTA Constraint for Multirotor eVTOL in Urban Air Mobility." Journal of Aerospace Information Systems, 16(7), pp.263-277. doi:10.2514/1.I010710.

[5] Pradeep, P., and Wei, P., "Energy optimal speed profile for arrival of tandem tilt-wing eVTOL aircraft with RTA constraint." In 2018 IEEE CSAA Guidance, Navigation and Control Conference (CGNCC), pp. 1-6. doi: 10.1109/GNCC42960.2018.9018748.

[6] Pradeep, P., and Wei, P., "Heuristic Approach for Arrival Sequencing and Scheduling for eVTOL Aircraft in On-Demand Urban Air Mobility," In 2018 IEEE/AIAA 37th Digital Avionics Systems Conference (DASC), London, 2018, pp. 1-7. doi: 10.1109/DASC.2018.8569225.

[7] Thipphavong, D.P., Apaza, R., Barmore, B., Battiste, V., Burian, B., Dao, Q., Feary, M., Go, S., Goodrich, K.H., Homola, J. and Idris, H.R., 2018., "Urban air mobility airspace integration concepts and considerations." In 2018 Aviation Technology, Integration, and Operations Conference 2018, p. 3676. doi: 10.2514/6.2018-3676.

[8] Mueller, E. R., Kopardekar, P. H., and Goodrich, K. H., "Enabling airspace integration for high-density on-demand mobility operations." In 17th AIAA Aviation Technology, Integration, and Operations Conference, p. 3086. 2017. doi:110.2514/6.2017-3086.

[9] Airbus-A3, "Vahana Aero," https://vahana.aero/, 2018. [Online; accessed 18-January-2019].

[10] Snyder, C. A., "Personal rotorcraft design and performance with electric hybridization," 2017, https://ntrs.nasa.gov/archive/nasa/casi.ntrs.nasa.gov/20170005655.pdf [accessed 18 Jan. 2019].

[11] Kim, H. D., Perry, A. T., and Ansell, P. J., "A review of distributed electric propulsion concepts for air vehicle technology," In 2018 AIAA/IEEE Electric Aircraft Technologies Symposium (EATS), AIAA Paper 2018-4998, 2018. doi:10.2514/6.2018-4998

[12] EHang-184, "EHANG 184 autonomous aerial vehicle specs," http://www.ehang.com/ehang184/specs/, 2018. [Online; accessed 18-January-2019].

[13] Volocopter, "Volocopter technical features," https://www.volocopter.com/en/urban-mobility/, 2018. [Online; accessed 18-January-2019].

[14] Bosson, C., and Lauderdale, T. A., "Simulation evaluations of an autonomous urban air mobility network management and separation service." In 2018 Aviation Technology, Integration, and Operations Conference, p. 3365. doi: 10.2514/6.2018-3365.

[15] Prevot, T., Rios, J., Kopardekar, P., Robinson III, J. E., Johnson, M., and Jung, J., "UAS traffic management (UTM) concept of operations to safely enable low altitude flight operations." In 16th AIAA Aviation Technology, Integration, and Operations Conference, p. 3292. doi:10.2514/6.2016-3292.

[16] Hong, Y., Lee, S., Lee, K., and Kim, Y., "Optimal scheduling algorithm for air traffic point merge system using MILP." In 2018 Advances in Aerospace Guidance, Navigation and Control, pp. 407-420. Springer, Cham. doi:10.1007/978-3-319-65283-2_22.

[17] Pawelek, A., Dalmau Codina, R., Lichota, P., and Prats Menendez, X., "Arrival traffic synchronisation with Required Time of Arrivals for fuel-efficient trajectories." In 2017 Proceedings of the 17th ATIO-AIAA Aviation Technology, Integration, and Operations Conference, pp. 1-14. doi: 10.2514/6.2017-3770.

[18] Neuman, F., and Erzberger, H., "Analysis of sequencing and scheduling methods for arrival traffic." `https://ntrs.nasa.gov/archive/nasa/casi.ntrs.nasa.gov/19900014057.pdf`, (1990). [Online; accessed 18-January-2019].

[19] Erzberger, H. and Itoh, E., "Design principles and algorithms for air traffic arrival scheduling." (2014)." `https://ntrs.nasa.gov/archive/nasa/casi.ntrs.nasa.gov/20140010277.pdf`, (2014). [Online; accessed 18-January-2019].

[20] Vascik, P.D. and Hansman, R.J., "Development of vertiport capacity envelopes and analysis of their sensitivity to topological and operational factors." In AIAA Scitech 2019 Forum, p. 0526. 2019. doi: 10.2514/6.2019-0526.

[21] Anagnostakis, I., Clarke, J. P., Bohme, D., and Volckers, U., "Runway operations planning and control: Sequencing and scheduling." In System Sciences, 2001. Proceedings of the 34th Annual Hawaii International Conference on (pp. 12-pp). IEEE. doi:10.1109/HICSS.2001.926330.

[22] Malik, W., and Jung, Y. C., "Exact and heuristic algorithms for runway scheduling." In 16th AIAA Aviation Technology, Integration, and Operations Conference, p. 4072. 2016. doi:10.2514/6.2016-4072.

[23] Balakrishnan, H., and Chandran, B., "Algorithms for scheduling runway operations under constrained position shifting." Operations Research 58, no. 6 (2010): 1650-1665. doi:10.1287/opre.1100.0869.

[24] Balakrishnan, H., and Chandran, B., "Scheduling aircraft landings under constrained position shifting." In AIAA guidance, navigation, and control conference and exhibit, p. 6320. 2006. doi:10.2514/6.2006-6320.

[25] Lee, H., and Balakrishnan, H., "A study of tradeoffs in scheduling terminal-area operations." Proceedings of the IEEE, 96(12), 2081-2095. doi:10.1109/JPROC.2008.2006145.

[26] Kulkarni, C., Schumann, J., and Roychoudhury, I., "On-board battery monitoring and prognostics for electric-propulsion aircraft." In 2018 AIAA/IEEE Electric Aircraft Technologies Symposium, AIAA Propulsion and Energy Forum, (AIAA 2018-5034). doi:10.2514/6.2018-5034.

[27] Alnaqeb, A.H., Li, Y., Lui, Y.H., Pradeep, P., Wallin, J., Hu, C., Hu, S. and Wei, P., "Online prediction of battery discharge and flight mission assessment for electrical rotorcraft", 2018 AIAA Aerospace Sciences Meeting, AIAA SciTech Forum, (AIAA 2018-2005). doi:10.2514/6.2018-2005.

[28] Zhan, Z. H., Zhang, J., Li, Y., Liu, O., Kwok, S. K., Ip, W. H., and Kaynak, O., "An efficient ant colony system based on receding horizon control for the aircraft arrival sequencing and scheduling problem." IEEE Transactions on Intelligent Transportation Systems 11, no. 2 (2010): 399-412. doi:10.1109/TITS.2010.2044793.

[29] Hu, X. B., and Chen, W. H., "Genetic algorithm based on receding horizon control for arrival sequencing and scheduling." Engineering Applications of Artificial Intelligence 18, no. 5 (2005): 633-642. doi:10.1016/j.engappai.2004.11.012.

[30] Psaraftis, H. N., "A dynamic programming approach for sequencing groups of identical jobs." Operations Research 28, no. 6 (1980): 1347-1359. doi:10.1287/opre.28.6.1347.

[31] Dear, R. G., "The dynamic scheduling of aircraft in the near terminal area." Cambridge, Mass.: Flight Transportation Laboratory, Massachusetts Institute of Technology,[1976].

[32] Patterson, M. A., and Rao, A. V., "GPOPS-II: A MATLAB software for solving multiple-phase optimal control problems using hp-adaptive Gaussian quadrature collocation methods and sparse nonlinear programming." ACM Transactions on Mathematical Software (TOMS), 41(1), 1. doi:10.1145/2558904.

[33] Wachter, A., and Biegler, L. T., "On the implementation of an interior-point filter line-search algorithm for large-scale nonlinear programming." Mathematical programming, 106(1), 25-57. doi:10.1007/s10107-004-0559-y.

[34] Donohue, G.L. and Laska, W.D., "United States and European airport capacity assessment using the GMU macroscopic capacity model." Progress in Astronautics and Aeronautics 193 (2001): 61-76.

[35] Guerreiro, N.M., Hagen, G.E., Maddalon, J.M. and Butler, R.W., “Capacity and throughput of urban air mobility vertiports with a first-come, first-served vertiport scheduling algorithm.” In AIAA Aviation 2020 Forum, American Institute of Aeronautics and Astronautics, 2020. doi:10.2514/6.2020-2903

[36] Meindl, B., and Templ, M., "Analysis of commercial and free and open source solvers for linear optimization problems." Eurostat and Statistics Netherlands within the project ESSnet on common tools and harmonised methodology for SDC in the ESS, 20.

[37] Willemain, T. R., Fan, H., and Ma, H., "Statistical analysis of intervals between projected airport arrivals." Rensselaer Polytechnic Inst., DSES Tech. Rept, 38-04.

[38] Van Rossum, G., and De Boer, J., "Interactively testing remote servers using the python programming language", CWI Quarterly, Volume 4, Issue 4 (December 1991), Amsterdam, pp 283-303.

[39] Verma, S., Keeler, J., Edwards, T.E. and Dulchinos, V., "Exploration of near term potential routes and procedures for urban air mobility." In AIAA Aviation 2019 Forum, p. 3624. 2019. doi:10.2514/6.2019-3624.